LA-UR -93-268

Los Alamos National Laboratory is operated by the University of California for the United States Department of Energy under contract W-7405-ENG-36.

TITLE: SIMPLIFIED DYNAMIC BUCKLING ASSESSMENT OF STEEL CONTAINMENTS

AUTHOR(S): Charles Farrar, MEE-13
Thomas Duffey, MEE-13 (Consultant
Dirk Renick, Annapolis Naval Academy

SUBMITTED TO: 12th Internatioal Conference on Structural Mechanics
in Reactor Technology
Stuttgart, Germany
Aug. 15-20, 1993

DISCLAIMER

Los Alamos Los Alamos National Laboratory
Los Alamos, New Mexico 87545

SIMPLIFIED DYNAMIC BUCKLING ASSESSMENT OF STEEL CONTAINMENTS

C. R. Farrar, T. A. Duffey, and D. H. Renick

Los Alamos National Laboratory, Los Alamos, NM 87545 USA

ABSTRACT

A simplified, three-degree-of-freedom analytical procedure for performing a response spectrum buckling analysis of a thin containment shell is developed. Two numerical examples with R/t values which bound many existing steel containments are used to illustrate the procedure. The role of damping on incipient buckling acceleration level is evaluated for a regulatory seismic spectrum using the two numerical examples. The zero-period acceleration level that causes incipient buckling in either of the two containments increases 31% when damping is increased from 1% to 4% of critical. Comparisons with finite element results on incipient buckling levels are favorable.

1. INTRODUCTION AND SUMMARY

Metal containment structures for nuclear reactors are typically thin-walled shells that may be sensitive to buckling caused by a combination of conventional live and dead loads and by seismic excitation. While finite element methods are available for numerically evaluating the detailed dynamic response of such containments, these methods can be computationally tedious.* Simplified methods would be useful for rapidly obtaining estimates during the preliminary design phase and for assessing the margin to failure of existing containments.

This paper presents a simplified three-degree-of-freedom (3-DOF) analytical procedure for performing a response spectrum buckling analysis of a thin containment shell. Two numerical examples are then given illustrating the application of the analytical procedure, based upon containment R/t values of 450 and 645. These values bound the R/t values of many existing steel containments[1].

The role of damping on the incipient buckling acceleration level is evaluated based on the simple 3-DOF modal/response spectrum analysis procedure and on a site-independent seismic spectrum. The zero-period acceleration (ZPA) level that causes incipient buckling in either of the two containments analyzed increases 31% when damping is increased from 1% to 4% of critical.

2. SIMPLIFIED BUCKLING ANALYSIS

2.1 Simplified Model

*Containment shells analyzed in a companion paper (Ref. 1) using the finite element method with transient-time integration required 6-10 hrs. CPU time per analysis on a CRAY Y-MP computer for a 6 sec. time history of response.

The 3-DOF model of the containment is shown in Fig. 1. The first DOF is horizontal motion, similar to that of a short cantilever beam, and results from the shear-bending mode of response. The second DOF is identical to the first, but acts in the orthogonal horizontal direction (not shown in Fig. 1). The third DOF corresponds to axial motion in the vertical direction. Referring to Fig. 1, m denotes either m_h or m_v, where m_h is the participating mass for the horizontal translation mode and m_v is the participating mass for the vertical translation mode. In both cases, the participating mass is assumed to be concentrated at the end of the cylindrical portion of the containment.

2.2 Determination of Resonant Frequencies

The resonant frequency for the vertical translational mode, f_v, is estimated as

$$f_V = \frac{1}{2\pi}\sqrt{\frac{K_V}{m_V}}, \tag{1}$$

where K_V is the axial stiffness of the cylindrical shell. These quantities are defined as

$$K_v = AE/L, \text{ and} \tag{2}$$

$$m_V = m_{sp} + 1/3\, m_c, \tag{3}$$

where m_{sp} = the mass of the hemispherical dome; m_c = the mass of the cylindrical portion of the containment; E = Young's modulus; A = Cross-sectional area of cylindrical shell; and L = length of the cylindrical portion of the containment. The participating mass for vertical motion, m_V, was determined by Rayleigh's Method [2].

Because the structure is modeled as axisymmetric, the two shear-bending modes associated with the horizontal DOFs will have the same resonant frequency. This frequency, f_h, is estimated as

$$f_h = \frac{1}{2\pi}\sqrt{\frac{K_h}{m_h}}, \text{ and} \tag{4}$$

$$K_h = \frac{1}{\frac{L^3}{3EI} + \frac{L}{\kappa AG}}, \tag{5}$$

where I = the cross-section area moment of inertia; κ = a shape factor for thin circular cross-sections, 2.0; and G = the shear modulus.

The containment is similar to a short beam; hence, the horizontal displacement of the cylinder, when responding in its fundamental shear-bending mode, is assumed to be a linear function of the height of the cylinder. Using this assumed displacement field, Rayleigh's method is again employed to determine m_h, the participating mass for the shear-bending modes. If the mass of the hemisphere is lumped at the hemisphere's centroid, then the participating mass for each shear-bending mode is

$$m_h = \frac{m_c}{3} + m_{sp}\left(1 + \frac{2a}{L} + \left(\frac{a}{L}\right)^2\right) \qquad (6)$$

where a = the height of the hemisphere's centroid above the top of the cylindrical portion of the containment.

2.3 Dynamic Amplification

A standard site-independent response spectra, Fig. 2 (NRC Regulatory Guide 1.60[3]), is next used to determine the dynamic amplification factors associated with these three modes.

2.4 Stresses from Simple Beam Theory

The maximum axial stress at the base of the cylindrical shell is next determined from beam theory. Axial stress caused by bending induced from the horizontal component of acceleration is considered, along with the axial stress caused by the static load of the containment, including typical normal operating negative air pressure effects and the axial stress caused by the vertical inertial loading. These stress components are as follows:

$$\sigma_{\phi_{Dyh}} = \frac{Mc}{I} \qquad \sigma_{\phi_{Dyv}} = \frac{P_{Dy}}{A} \qquad \sigma_{\phi_{St}} = \frac{P_{St}}{A} + \frac{pr}{2t} \qquad (7)\text{-}(9)$$

where $\sigma_{\phi_{Dyh}}$ = the longitudinal dynamic stress that results from the horizontal inertial force; $\sigma_{\phi_{Dyv}}$ = the longitudinal dynamic stress that results from the vertical inertial force; $\sigma_{\phi_{St}}$ = the longitudinal static stress; M = the bending moment at the containment base caused by the horizontal inertial force; P_{St} = longitudinal static load; P_{Dy} = longitudinal inertial load; p = the negative air pressure during normal operating conditions; c = distance from the neutral axis to the outermost fiber; r = radius of the cylindrical portion of the containment; and t = the wall thickness of the containment shell.

The bending moment appearing above is determined from

$$M = D_{Ah}\, g\, m_h L, \qquad (10)$$

where D_{Ah} = dynamic amplification factor for the horizontal translation mode, and g = horizontal acceleration.

The axial static load is given by

$$P_{St} = m_t g_o, \qquad (11)$$

where $m_t = m_{sp} + m_c$, and g_0 = the acceleration caused by gravity.

Finally, the axial inertial load is given by

$$P_{Dy} = 0.67 D_{Av} g m_o, \qquad (12)$$

where D_{Av} = Dynamic amplification factor for the vertical translation mode, and 0.67 is a factor that relates the vertical acceleration to the horizontal acceleration [3].

2.5 Shear Buckling Considerations

The maximum in-plane shear stress in the cylindrical shell occurs at a position ± 90° around the shell from the point of maximum compressive stress. Based on [4], for a cantilever cylindrical shell loaded by a transverse concentrated force, P, on its end, it can be shown that the maximum shear stress is

$$\left(\sigma_{\phi\theta}\right)_{Max} = \frac{P}{\pi r t}. \tag{13}$$

The horizontal shear force is given by

$$P = D_{Ah}\, g\, m_h. \tag{14}$$

Combining Eqs. (13) and (14) results in

$$\sigma_{\phi\theta_{Dy}} = \frac{D_{Ah}\, g\, m_h}{\pi r t}. \tag{15}$$

Note that this component of stress results from the dynamic loads caused by the horizontal component of the seismic excitation.

2.6 Circumferential Stresses

The simplified 3-DOF model is effectively a beam-column representation of a shell. It does not, therefore, account for circumferential stresses, θ, induced by the seismic input accelerations. The role of these circumferential (hoop) stresses is significant on the value of g-loading which corresponds to incipient buckling [1]. A "hoop stress reduction factor" to be used to correct for this shortcoming of the simplified model was therefore determined numerically. Finite element calculations were performed using the containment shell models (R/t = 450, 645) described in a companion paper [1]. A variety of earthquake acceleration-time histories were used as inputs to the computer models. Using procedures of [1], the incipient g-loading which just leads to buckling was determined for both shell models and each of the seismic input signals (the signals were selected such that a large range in amplifications of the fundamental shear-bending modes of the two models would be achieved). Then the corresponding g-loading for buckling was determined assuming σ_θ was zero. The ratio of these buckling g-values is the hoop stress reduction factor which, when multiplied by the 2-dimensional incipient buckling value predicted by this simplified 3-DOF model, corrects for the absence of the circumferential stress in the interaction equations.

The resulting hoop stress reduction factor is plotted in Fig. 3, where it is seen that the factor is reasonably independent of the amplification factor of the shear-bending modes of the two shells. A hoop stress reduction factor of 0.6 appears to reasonably approximate the data for both shells.

2.7 Combining Stress Components

The stress components can be combined assuming three components of input are acting simultaneously. To account for random phasing of the earthquake input components, a 100-40-40 rule for combining seismic stresses was used [5]. The stress interaction curve from ASME Code Case N-284 [6] is then utilized to evaluate buckling. For axial compression and shear, the interaction curve reduces to

$$\frac{\sigma_\phi}{\sigma_{\phi_D}} + \left(\frac{\sigma_{\phi\theta}}{\sigma_{\phi\theta_D}}\right)^2 = 1 \tag{16}$$

where subscript D denotes intercept values of limiting axial and shear stress [6]. Two critical locations at the base of the containment must be considered. These points are shown in Fig. 4. Point 1 in Fig. 4 will experience the maximum longitudinal stress, while Point 2 will experience the maximum in-plane shear stress.

3. NUMERICAL EXAMPLES

Using the above procedures and ASME Code Case N-284, the buckling capacity of the two (R/t = 645 and 450) unstiffened containment shells are determined for different levels of viscous damping. Details of geometry, material and loading, as well as intermediate results, are presented elsewhere [7]. A scaling procedure also detailed in [7] is utilized to determine the zero-period acceleration (ZPA) values that correspond to incipient buckling for a generic state of stress.

Resulting values of the ZPA that lead to a condition of incipient buckling as defined by ASME Code Case N-284 are summarized in Table 1 for the two containment examples. Note that the hoop stress reduction factor of 0.6 has been applied to the results in Table 1.

As can be seen in these numerical examples, incipient buckling level is increased by 31% in both cases as the damping is increased from 1% to 4%.

4. COMPARISON WITH FINITE ELEMENT RESULTS

Results of finite element calculations of incipient buckling levels for the same two numerical examples as presented herein are taken from a companion paper [1]. Comparisons of g-levels are presented in Table 2. Comparisons identified as "two dimensional" are those for which transient hoop stresses are not included (See Section 2.6). "Three dimensional" comparisons include hoop stresses (using the factor 0.6 in the case of the 3-DOF solution). Agreement for the 3-DOF solution and finite element solutions is within 25% for the 3 dimensional comparisons.

5. RESULTS AND CONCLUSIONS

A simplified three-degree-of-freedom analytical procedure is presented for performing a response spectrum buckling analysis of a thin containment shell. The procedure is consistent with US NRC Seismic Analysis Guidelines and the ASME PVP Code Case N-284 Containment Buckling Procedures.

Based on the above procedure, two numerical examples are utilized to evaluate the role of damping on incipient seismic buckling. The zero-period acceleration level that causes incipient buckling in either of the two containments analyzed increases 31% when damping is increased from 1% to 4% of critical for the regulatory spectra considered.

Comparisons with tedious finite element results are within 25%, suggesting that the approximate procedure outlined herein may be suitable for preliminary containment buckling design estimates.

REFERENCES

1. Farrar, C. R., Duffey, T. A., Goldman, P.A., and Bennett, J.G. 1993. "Dynamic Buckling of Containments: The Influence of Damping". Proceedings of the 12th International Conference on Structural Mechanics in Reactor Technology, Volume J, Paper 10/2.

2. Thomson, W. T. 1981. Theory of Vibration with Applications, Englewood Cliffs: Prentice-Hall, Inc., pp. 196-197.

3. U.S. AEC Regulatory Guide 1.60. 1973. "Design Response Spectra for Seismic Design of Nuclear Power Plants, Rev. 1". U.S Atomic Energy Commission. Washington, D.C.

4. Lu, S. Y. 1965. "Buckling of Cantilever Cylindrical Shell with a Transverse End Load," AIAA Journal, 3, No. 12.

5. "Seismic Analysis of Safety-Related Nuclear Structures and Commentary on Standard for Seismic Analysis of Safety Related Nuclear Structures". 1986. ASCE 4-86, American Society of Civil Engineers, New York.

6. ASME Boiler and Pressure Vessel Code, Section III. 1980. Division 1, Case N-284, "Metal Containment Shell Buckling Design Methods". Approval date: August 25.
7. Farrar, C. R., Duffey, T. A., Goldman, P.A., and Bennett, J. G. 1992. "Seismic Buckling Capacity of Unstiffened, Free-Standing Steel Containments". LA-12359-MS. Los Alamos National Laboratory, Los Alamos, NM, USA.

TABLE 1. ZERO PERIOD ACCELERATION VALUES THAT WILL CAUSE AN INCIPIENT BUCKLING CONDITION USING REG. GUIDE 1.60 SPECTRA

Damping	R/t = 645	R/t = 450
1%	0.16 g's	0.35 g's
2%	0.17 g's	0.38 g's
4%	0.21 g's	0.46 g's

TABLE 2. COMPARISON OF LUMPED MASS AND FINITE ELEMENT RESULTS USING REG. GUIDE 1.60 SPECTRUM

R/t	Damping	Two Dimensional Lumped Mass No Hoop Stress	FEM- No Hoop Stress	Three Dimensional Lumped Mass With Hoop Stress	FEM With Hoop Stress
645	1%	0.26 g's	0.26 g's	0.16 g's	0.19 g's
645	2%	0.29 g's	0.29 g's	0.17 g's	0.22 g's
645	4%	0.35 g's	0.34 g's	0.21 g's	0.25 g's
450	1%	0.58 g's	0.39 g's	0.35 g's	0.27 g's
450	2%	0.63 g's	0.44 g's	0.38 g's	0.30 g's
450	4%	0.77 g's	0.52 g's	0.46 g's	0.36 g's

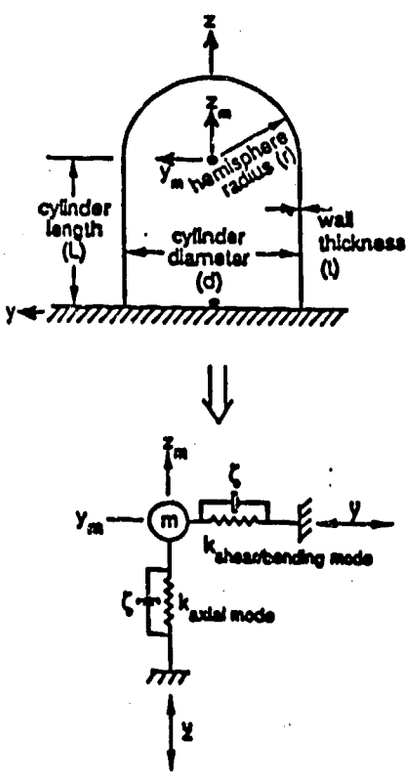

Fig. 1 Three degree-of-freedom idealization of a containment structure.

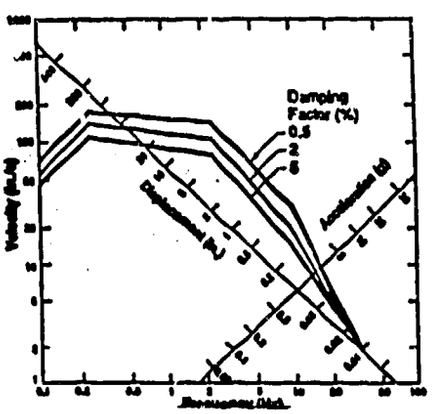

Fig. 2 Site-independent response spectra from Reg. Guide 1.60 (Adapted from [3]).

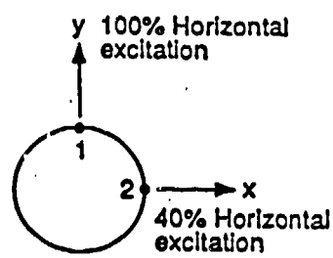

Fig. 4 Points at the base of the containment for which buckling interaction equations were considered.

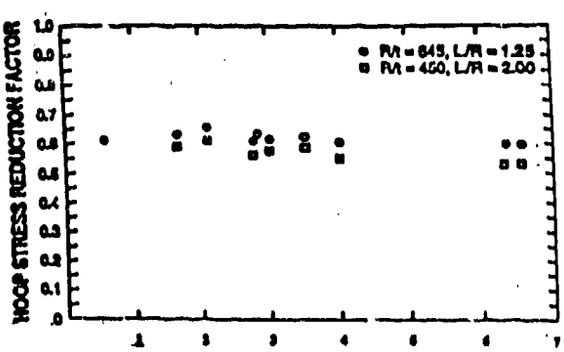

Fig. 3 Hoop stress reduction factor determined numerically.